The effect of initial vortex asymmetric structure on tropical cyclone intensity change in response to an imposed environmental vertical wind shear

Qi Gao[a,b] and Yuqing Wang[c]

[a]Department of Atmospheric and Ocean Sciences, Institute of Atmospheric Sciences, Fudan University, Shanghai, China

[b]State Key Laboratory of Severe Weather, Chinese Academy of Meteorological Sciences, China Meteorological Administration, Beijing, China

[c]International Pacific Research Center and Department of Atmospheric Sciences, School of Ocean and Earth Science and Technology, University of Hawaii at Manoa, Honolulu, HI, USA

August 2, 2023 (revised)

Dateline

Key Points:

- The initial asymmetric structure in a TC vortex can either enhance or suppress the TC weakening induced by an imposed environmental VWS.
- If the initial asymmetric structure is in phase with the VWS-induced asymmetric structure, the TC weakening would be enhanced and vice versa.
- The TC asymmetric structure should be better observed in real time and realistically represented in numerical weather prediction models.

Resubmitted to ***Geophysical Research Letters***

Corresponding author: Yuqing Wang, yuqing@hawaii.edu

Abstract

Previous studies have investigated how the environmental vertical wind shear (VWS) may trigger the asymmetric structure in an initially axisymmetric tropical cyclone (TC) vortex and how TC intensity changes in response. In this study, the possible effect of the initial vortex asymmetric structure on the TC intensity change in response to an imposed environmental VWS is investigated based on idealized full-physics model simulations. Results show that the effect of the asymmetric structure in the initial TC vortex can either enhance or suppress the initial weakening of the TC in response to the imposed environmental VWS. When the initial asymmetric structure is in phase of the VWS-induced asymmetric structure, the TC weakening will be enhanced and vice versa. Our finding calls for realistic representation of initial TC asymmetric structure in numerical weather prediction models and observations to better resolve the asymmetric structure in TCs.

Plain language summary

Although a strong tropical cyclone (TC) is often treated as an axisymmetric vortex in most theoretical studies, asymmetric structure always exists in a TC in nature, such as that generated by the environmental vertical wind shear (VWS). However, it is unclear whether and how the asymmetric structure in the initial TC vortex may affect the TC intensity change in response to an imposed environmental VWS. This has been addressed in this study by conducting idealized high-resolution numerical simulations. Results show that the asymmetric structure in the initial TC vortex can either enhance or suppress the initial weakening of the TC in response to an imposed environmental VWS depending on how the initial asymmetry is aligned with the asymmetry induced by the VWS. If they are in phase, the TC weakening would be enhanced and vice versa. Our finding highlights the importance of realistically representing the asymmetric structure in the initial TC vortex in numerical weather prediction models for TC forecasts and also the need to better resolve the TC asymmetric structure in observations.

1. Introduction

A strong tropical cyclone (TC) is often considered to be quasi-axisymmetric with relatively weak embedded asymmetric structure, therefore, it is common to assume a TC as an axisymmetric vortex in previous theoretical and numerical modeling studies on TC intensification and maximum potential intensity (e.g., Ooyama, 1969; Emanuel, 1986, 2012; Rotunno & Emanuel, 1987; Bryan & Rotunno, 2009a, b; Li et al., 2019, 2020, 2021, 2022; Wang et al., 2021a, b, 2023). Furthermore, our current understanding on TC development has also been largely based on the axisymmetric processes, such as the conditional instability of the second kind (CISK), the wind-induced surface heat exchange (WISHE), and the balanced TC vortex dynamics (Charney & Eliassen, 1964; Ooyama, 1969; Schubert & Hack, 1982; Emanuel et al., 2004; Wang & Wu, 2004), although the asymmetric processes may play critical roles in TCs (e.g., Montgomery et al., 2006; Nolan et al., 2007; Montgomery & Smith, 2014).

Asymmetric structures in a TC are often unfavorable for TC intensification. One example is asymmetry caused by TC internal dynamics, such as vortex Rossby waves and mesovortices in the eyewall, which play some roles in limiting TC intensity by eddy mixing across the eyewall or affecting the slope of the eyewall ascent (Wang, 2002a, b, 2007, 2009; Yang et al., 2007; Persing et al., 2013). The asymmetric structure in a TC can also be induced by external environmental forcing. One of such examples is the environmental vertical wind shear (VWS, Jones, 1995; Wang & Holland, 1996a; Frank & Ritchie, 2001; Li et al., 2008, 2017; Xu & Wang, 2013; Gu et al., 2018; Li et al., 2017; Li & Dai, 2019; Fu et al., 2019; Gao et al., 2020). The VWS could perturb the thermal wind balance of the TC and cause the vertical tilt of the TC vortex, leading to the asymmetric vertical motion in the eyewall (Jones, 1995; Wang & Holland, 1996a; Frank & Ritchie, 2001; Xu & Wang, 2013). Environmental VWS can also trigger the development of outer spiral rainbands mainly in the downshear quadrants (Heymsfield et al. 2006; Riemer & Montgomery, 2011; Li et al., 2017). In addition, different directions of environmental VWS may have different impacts on TC intensity changes (He et al., 2015; Gu et al., 2019). Zeng et al. (2010) found that for similar VWS magnitudes, an easterly VWS was preferable to a westerly VWS for TC intensification, which was explained by the superimposed beta (meridional variation of the Coriolis parameter) effect (Ritchie & Frank, 2007; Wang & Holland, 1996b, c). Ritchie & Frank (2007) found that the beta effect can induce a weak northwesterly VWS over the TC core in the northern hemisphere. As a result, the effect of westerly (easterly) VWS on TC intensity change would be enhanced (suppressed) by beta-induced VWS.

Previous studies have mostly focused on how the asymmetric structure is triggered and how the triggered asymmetric structure affects TC intensity change (Wang, 2002a, b, 2009; Yang et al., 2007; Xu & Wang, 2013; Persing et al., 2013; Li & Dai, 2019). However, it is still a challenge to realistically initialize the inner-core asymmetric structure of a TC vortex in a numerical weather prediction model. It is also unknown how the predicted/simulated TC intensity change may be affected by the initial asymmetric structure in a numerical weather prediction model. For example, some dynamical vortex initialization schemes developed so far mainly spin up the axisymmetric vortex, and little attention has been given to the initial asymmetric vortex structure (Cha & Wang, 2013; Liu et al., 2018; Liu et al., 2019). Recently, Zhong et al. (2023) found that the spinup and spindown members in ensemble forecasts of TC intensity show oppositely phased distribution in their initial asymmetric wind fields, and they hypothesized that the phased relationships between the direction of VWS and eyewall convection might influence the TC intensity evolution. However, they did not examine the details.

In this study, we will show that the initial asymmetric structure of a TC vortex is key to the intensity change of a TC at different developing stages in response to an imposed environmental VWS. We will also demonstrate that the VWS-induced asymmetry could be either enhanced or suppressed by the asymmetric structure in the initial TC vortex depending on the relative phase and strength of the two asymmetric structures. Our finding can help understand why both spinup and spindown members coexist in ensemble forecasts of TC intensity by numerical weather prediction models (e.g., Zhong et al., 2023) and also calls for attention to adequately represent the asymmetric structure of the TC vortex in numerical models.

2. Model and experimental design

The three-dimensional, compressible, non-hydrostatic, full-physics Weather Research and Forecasting (WRF) model version 4.2.2 (Skamarock et al., 2008) was used to perform a series of numerical experiments. The horizontal model domain was triply nested with grid spacings of 18, 6 and 2 km and sizes of 502×361, 361×361, and 301×301 grid points, respectively. The two inner-meshes automatically moved following the model TC vortex center. The model atmosphere had sixty vertical levels with the model top at 25 km. The model physics included the Yonsei University planetary boundary layer scheme (YSU; Hong et al., 2006) and the Thompson cloud microphysics scheme (Thompson et al., 2008). The modified Tiedtke cumulus parameterization scheme (Tiedtke, 1989; Zhang et al., 2011) was only applied to the outermost mesh. Radiation was not considered for simplicity in this study.

Since the main concern in this study is to examine the effect of the asymmetric structure of the initial TC vortex on the response of TC intensity change to an imposed moderate environmental VWS, all numerical experiments were conducted on an *f*-plane at 15°N over the ocean with a uniform sea surface temperature of 28.5°C. The initial unperturbed sounding of the model atmosphere was the moist-tropical sounding documented in Dunion (2011). In a control experiment (CTRL), the initial TC vortex was axisymmetric in gradient and thermal wind balance as in Rotunno & Emanuel (1987) with a maximum tangential wind speed of 18 m s^{-1} near the surface at a radius of 90 km, and the model was run for 192 h. The moderate environmental VWS was set to 10 m s^{-1} initially in geostrophic wind and hydrostatic balances. The vertical profiles of the zonal wind corresponding to the easterly VWS and westerly VWS are given in Figure 1a. Namely, the environmental zonal wind increased from 0 m s^{-1} below 3.5 km height to 10 m s^{-1} above 12.0 km. Note that both easterly and westerly VWS were considered since the VWS effect on TC intensity change is theoretically independent of the shear direction on the *f*-plane.

In the VWS experiments, the VWS was imposed onto the TC vortex after 24, 48, 72, and 96 h of simulation in CTRL described above. Since the TC vortex from CTRL developed asymmetric structure even though there was no any asymmetric forcing, as studied in Wang (2007), two sets of VWS experiments were conducted. In one set, only the axisymmetric component of the TC vortex from CTRL was used in the corresponding VWS experiments, and in the other set, the TC vortex from CTRL was directly used in the VWS experiments. The axisymmetric component of the vortex was calculated as the azimuthal average for all prognostic variables, including all hydrometeors, in the WRF model. In total, 16 VWS experiments were performed, among them 4 easterly VWS and 4 westerly VWS experiments initialized with the axisymmetric components of the TC vortices after 24, 48, 72, and 96 h of simulation from CTRL, and 4 easterly VWS and 4 westerly VWS experiments initialized with the TC vortices directly after 24, 48, 72, and 96 h of simulation from CTRL. We named the axisymmetric and asymmetric experiments as "_AXI" and "_ASY" in suffixes and the easterly and westerly VWS experiments as "SHE" and "SHW" in prefixes, respectively. Therefore, the corresponding experiments were named SHE24_AXI (SHE24_ASY), SHE48_AXI (SHE48_ASY), SHE72_AXI (SHE72_ASY), SHE96_AXI (SHE96_ASY), and SHW24_AXI (SHW24_ASY), SHW48_AXI (SHW48_ASY), SHW72_AXI (SHW72_ASY), SHW96_AXI (SHW96_ASY), respectively. The TC vortex center was defined as the point with the largest azimuthally averaged maximum tangential wind speed at the given time. Note that the environmental wind profile was well maintained throughout the 96-h simulations in all VWS experiments (not shown).

3. Results

Previous studies have shown that the development of asymmetric structure is responsible for a TC to weaken in environmental VWS as already mentioned in Section 1. In particular, the TC vortex would develop a quasi-steady wavenumber-1 asymmetry in vertical motion and convection in the eyewall with enhanced upward motion and convection in the downshear-left quadrant when facing down the direction of the VWS (e.g., Jones, 1995; Wang & Holland 1996a). As such, if the initial asymmetric structure of the initial TC vortex is in phase with the VWS-induced wavenumber-1 asymmetric structure, the asymmetry of the TC vortex would be enhanced, and thus the weakening of the TC in response to the imposed VWS would be enhanced. To demonstrate this possible mechanism, we first analyze the initial asymmetric structure of the TC vortices in CTRL.

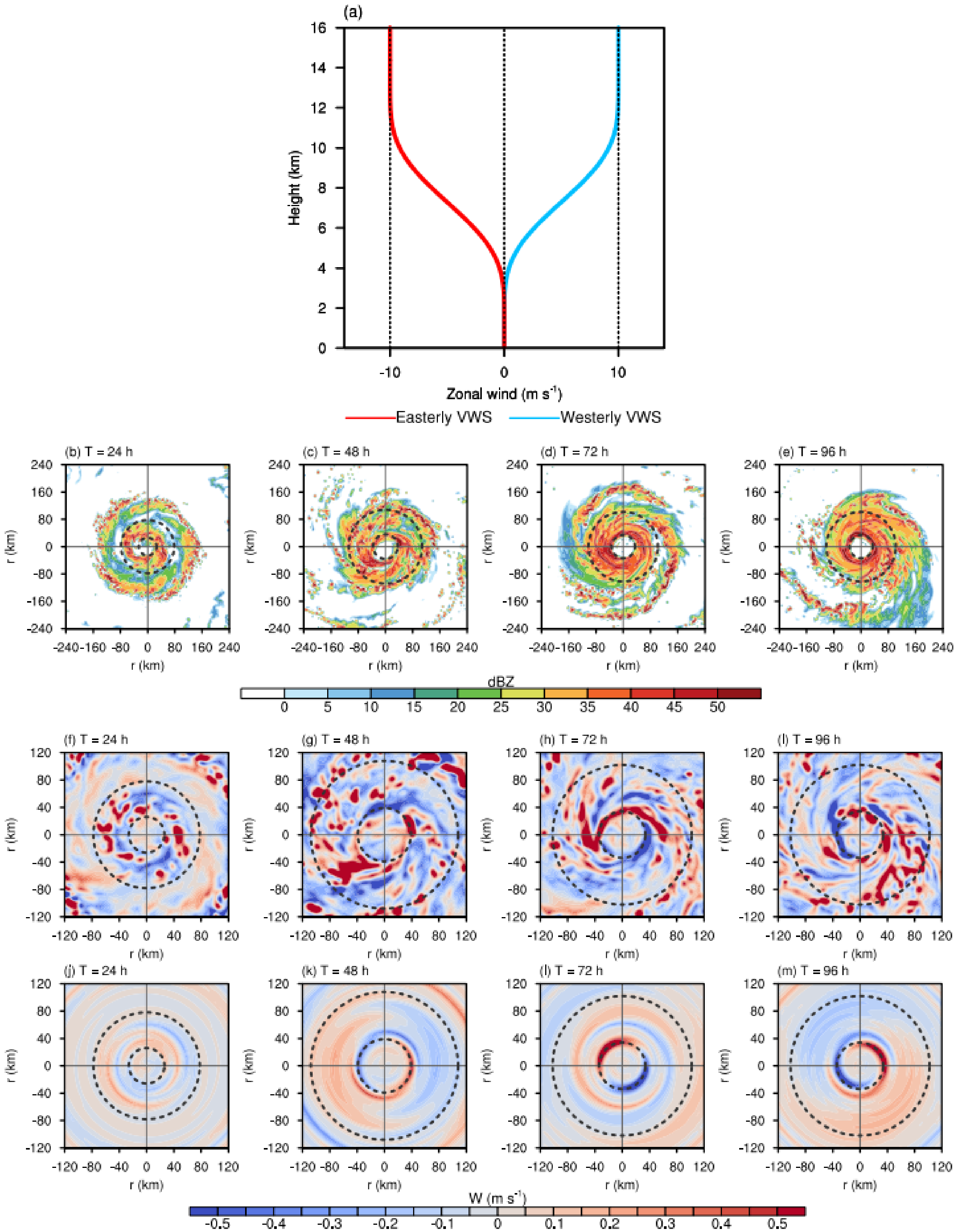

Figure 1. (a) The vertical profiles of the environmental zonal winds (red for easterly VWS and blue for westerly VWS) with the shear magnitudes of 10 m s^{-1}; (b-m) Horizontal distributions of radar reflectivity at 1-km height

(dBZ, the first row), the total (the second row) and wavenumber-1 (the third row) asymmetric vertical motion (m s^{-1}) averaged in the layer between 1–4 km heights. The area within the grey dashed big circle indicates the inner core and the small circle indicates the eyewall. The four vertical columns from the left to right correspond to times at 24, 48, 72, and 96 h of simulation in CTRL, respectively.

Figures 1b-1m shows the horizontal distribution of radar reflectivity at 1-km height and the total and wavenumber-1 asymmetric vertical motion computed by the azimuthal Fourier decomposition averaged in the layer between 1 and 4 km heights at the four times in CTRL when the TC vortex was used as the initial TC in the VWS experiments. The asymmetries arise at the four times in CTRL all from the TC internal dynamics. In the early development stage, the TC vortex is quite axisymmetric with relatively weak asymmetric structure in both radar reflectivity and vertical motion. The asymmetries in both fields become obvious by 48 h of the simulation, with upward asymmetric motion to the eastern semicircle and descending motion to the western semicircle. The asymmetries after 72 and 96 h of the simulation in CTRL become stronger but show different phases, with upward motion in the northwestern and subsidence in the southeastern quadrants by 72 h and upward motion in the eastern semicircle and subsidence in the western semicircle by 96 h. The asymmetries in vertical motion are dominated by wavenumber-1 structure (Figures 1j-1m), with large values mainly in the eyewall, about within the radius of maximum wind.

To examine the differences in the phase and strength of the asymmetric structure between the initial TC vortex and those induced by the imposed VWS, we now analyze the asymmetric structure of the TCs averaged within the first 1-3 hours of simulations after the VWS is imposed in the easterly VWS experiments with the initially axisymmetric TC vortex obtained from CTRL (Figure 2). Note that the asymmetric structure in the westerly VWS experiments is quite similar to that in the easterly VWS experiments for the initially axisymmetric TC vortex on the *f*-plane and thus not shown. We can see that a consistent predominant wavenumber-1 asymmetric structure developed in the first 3 h of simulations in all VWS experiments, with elevated radar reflectivity and upward motion downshear and downshear-left in the eyewall. Since the initial TC vortices were axisymmetric, the developed asymmetric structure in Figure 2 resulted primarily from the interaction between the TC vortex and the imposed VWS as documented in many previous studies (e.g., Frank & Ritchie, 2001; Xu & Wang, 2013). Note that the total and wavenumber-1 asymmetric vertical motion exhibit highly consistent features and dominated the total asymmetric vertical motion induced by the imposed environmental VWS.

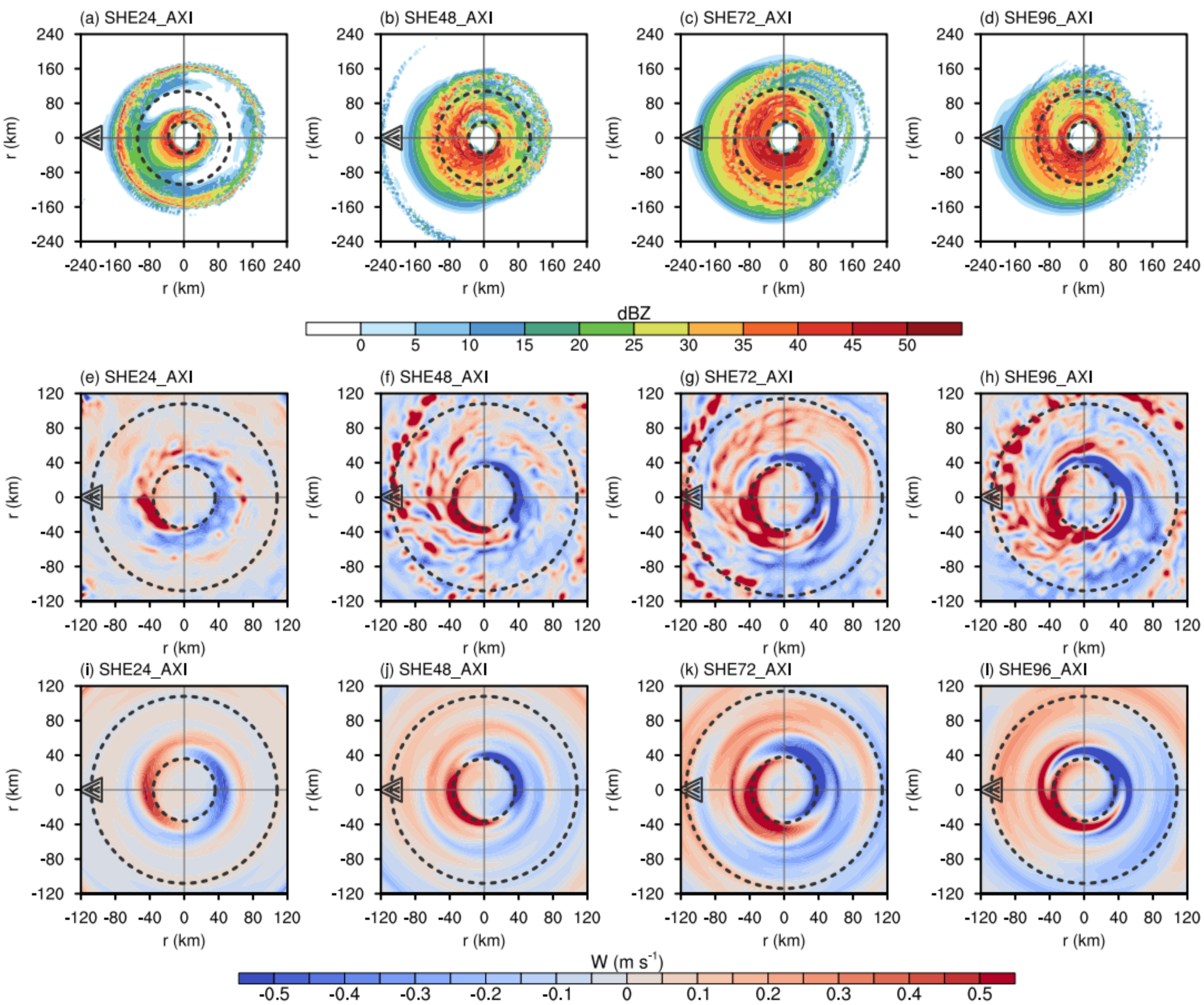

Figure 2. As in Figure 1b-m, but for the easterly VWS experiments with the initial axisymmetric TC vortices averaged within the first 1-3 hours of simulations after the VWS is imposed. The grey arrows indicate the direction of the environmental VWS.

Figure 3 shows the time evolutions of the TC intensity in terms of the central sea level pressure and the maximum wind speed in all VWS experiments initialized with the axisymmetric TC vortices from CTRL (colored in Figures 3a and 3c) and in those initialized with the TC vortices directly from CTRL (colored in Figures 3b and 3d), respectively. The TC in CTRL (black) intensified until 120 h of the simulation and evolved quasi-steadily afterwards. We can see from

Figures 3a and 3c that TCs experienced a reduced intensification rate when the VWS was imposed in the early intensification stage (for the TCs after 24 and 48 h of the simulation from CTRL) or a weakening when the VWS was imposed in the later intensification or mature stages (for the TCs after 72 and 96 h of the simulations from CTRL). This suggests that a moderate VWS had a relatively weak effect on the intensification of a weak TC. We hypothesize that for a weak TC, the weak warm core also indicates weak ventilation of the upper-level warm core by the imposed shear flow. However, for a relatively strong TC, in response to the imposed moderate VWS, the strong upper-level warm core implies relatively strong ventilation by the shear flow, resulting in a great weakening of the upper-level warm core and thus the weakening of the TC (Figure S1). A detailed process-oriented analysis of the TC intensity in response to the environmental VWS is planned for a future study. Here, we focus on the dependence of the response of the TC intensity change to the imposed moderate environmental VWS on the asymmetric structure of the initial TC vortex.

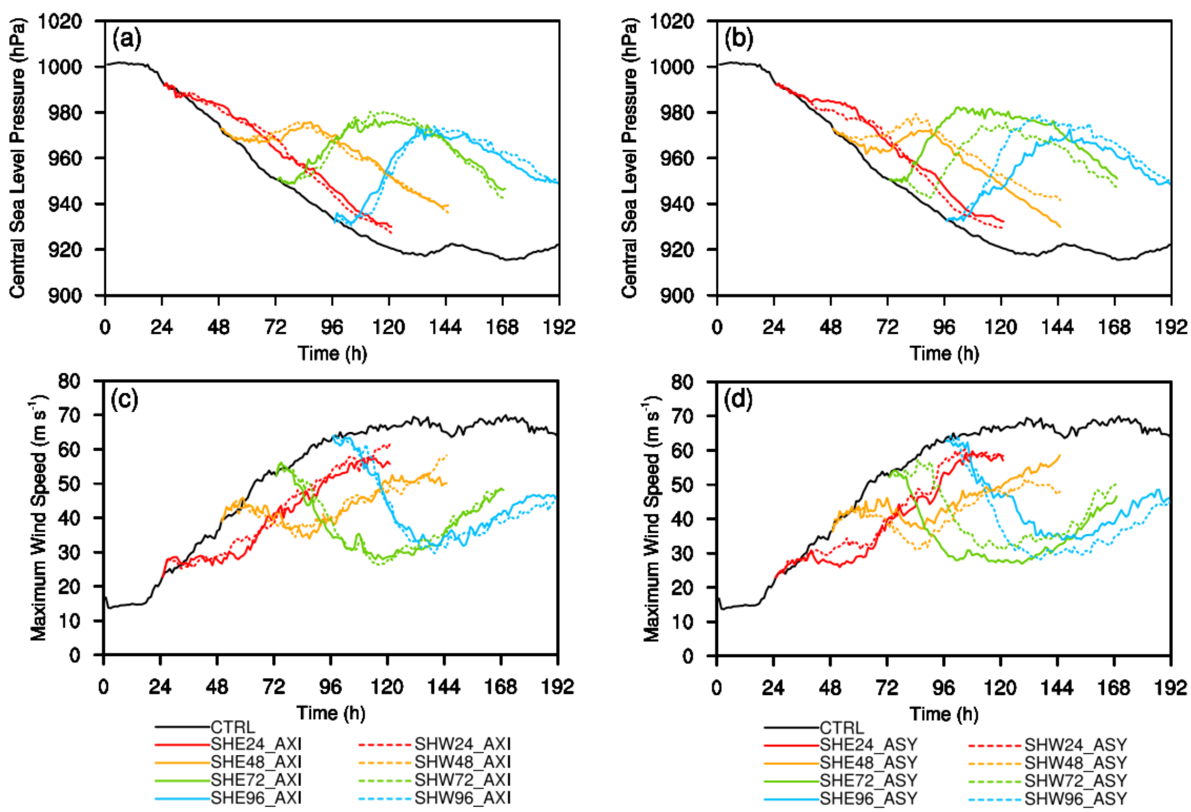

Figure 3. Time evolutions of (a, b) the simulated central sea level pressure (hPa) and (c, d) the maximum wind speed (m s^{-1}) of TCs in CTRL (black) and in all easterly (color solid) and westerly (color dashed) VWS experiments with initially axisymmetric vortex from CTRL (a, c) and with the TC vortex directly from CTRL (b,

d). The red, orange, green and blue colors represent the VWS experiments with TC vortices after 24, 48, 72, and 96 h of the simulation in CTRL, respectively.

As expected, the intensity evolutions (both the central sea level pressure and the maximum wind speed) for a TC with an initially axisymmetric structure embedded in westerly and easterly VWSs are quite similar on the *f*-plane (Figures 3a and 3c), as mentioned in section 2. Some small differences resulted from the small deviation of the initially axisymmetric TC vortex center from the center of the model domain and can be considered being unphysical and negligible. In contrast to the initially axisymmetric TC vortex, the TC vortex including both the axisymmetric and asymmetric structures from CTRL shows relatively large differences in intensity evolutions in responses to the imposed moderate environmental westerly and easterly VWSs (Figures 3b and 3d). Since the intensity evolution in environmental VWS on the *f*-plane experiment is little dependent on the direction of the VWS (Figure 3a and 3c), the large difference in intensity evolutions for a TC vortex embedded in easterly and westerly VWSs should result from the asymmetric structure of the TC vortex at the time of VWS was imposed. We can see from Figures 3b and 3d that the difference in TC intensity evolutions in the westerly and easterly experiments also depends on the stage of TC intensification in CTRL which show different degree of the asymmetric feature of the initial vortex. Although we found that the mean early TC weakening rate is nearly proportional to the degree of the asymmetry of the initial TC vortex, it also depends on the initial TC intensity. Therefore, the actual weakening of the TC in response to the imposed VWS could not be quantified with limited model experiments.

Comparing the asymmetric structures in Figures 1 and 2, we can see that the asymmetric structure in vertical motion at 72 h in CTRL resembles the asymmetric structure induced by easterly VWS for an initially axisymmetric TC vortex in Figure 2. The asymmetric distribution of vertical motion after 48 and 96 h of the simulation in CTRL is roughly in phase with that induced by the westerly VWS. As a result, the asymmetric structure in SHW48_ASY, SHW96_ASY, and SHE72_ASY would be enhanced due to the superposition of the in-phase asymmetric structure in the initial TC vortices. The enhanced asymmetric structure can lead to stronger upper-level ventilation, which is consistent with the larger weakening of TCs in SHW48_ASY, SHW96_ASY and SHE72_ASY as seen from Figures 3b and 3d.

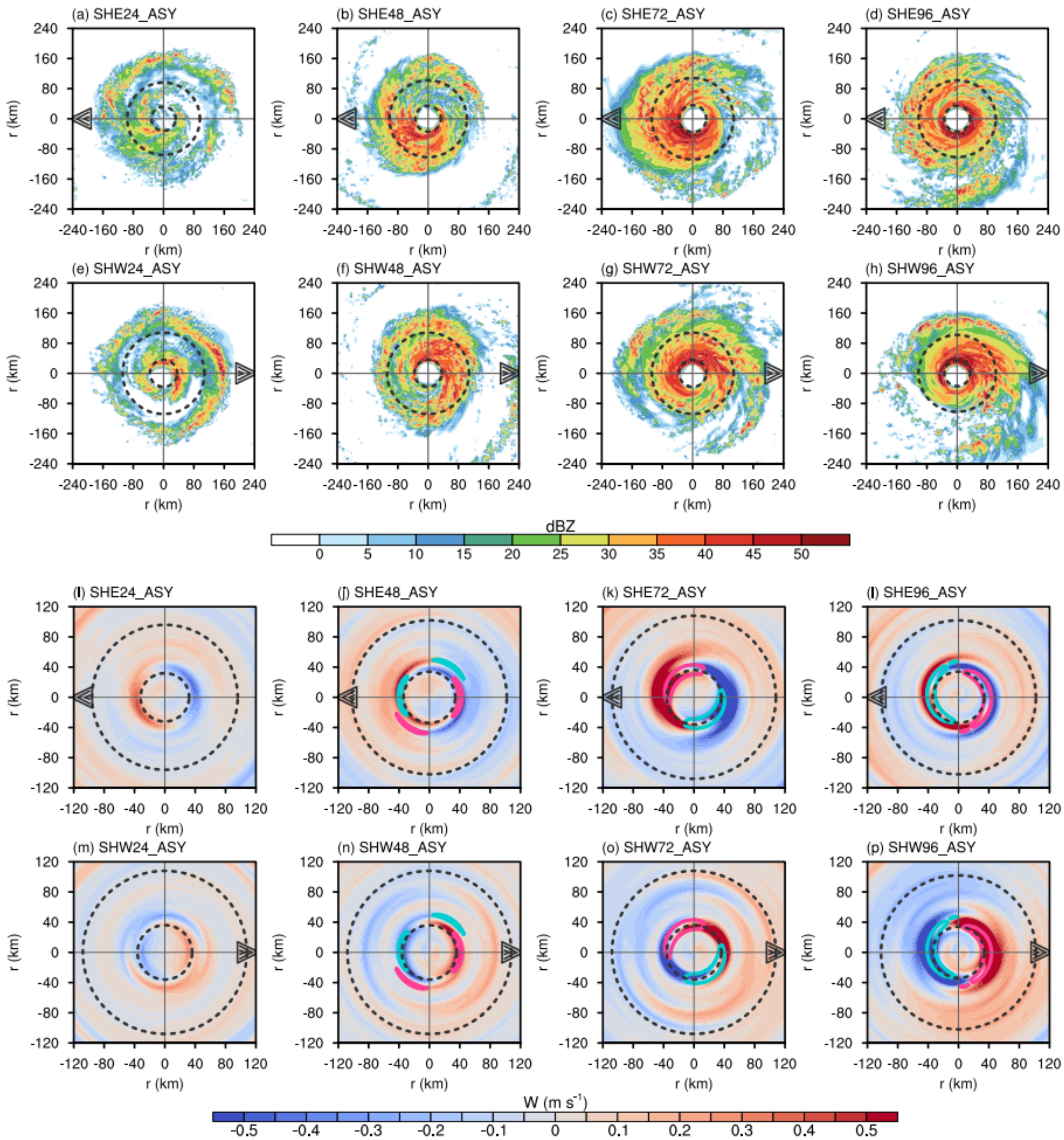

Figure 4. (a-h) and (i-p) are the same as in Figure 1b-e and 1j-m, respectively; but for the four easterly VWS and four westerly VWS experiments with the initial asymmetric TC vortices averaged within the first 1-3 hours of simulations after the VWS is imposed, respectively. The wavenumber-1 vertical motions (m s^{-1}) after 24, 48, 72, and 96 h of simulation in CTRL are overlaid in i-p contoured at -0.4 (blue) and 0.4 (pink) m s^{-1}. The grey arrows indicate the direction of the environmental VWS.

The above argument has been confirmed with the asymmetric structure in the 8 VWS experiments with the initially asymmetric TC vortex in Figure 4. As expected, although the phase of the wavenumber-1 asymmetric structure shows similarity in all VWS experiments, namely with upward motion downshear and downshear-left and subsidence upshear and upshear-right, the asymmetric structure in SHW48_ASY and SHW96_ASY was enhanced clearly among the westerly VWS experiments, especially in SHW96_ASY, while the asymmetric structure in SHE72_ASY was enhanced among the easterly VWS experiments. In contrast, the asymmetric structure in SHE48_ASY, SHE96_ASY, and SHW72_ASY was relatively weaker than that in SHW48_ASY, SHW96_ASY, and SHE72_ASY. As a result, the weakening of TCs in SHE48_ASY, SHE96_ASY, and SHW72_ASY was either suppressed or delayed compared to their corresponding opposite direction of shear (Figures 3b and 3d). These results strongly support our above hypothesis. Our finding demonstrates that the realistic representation of asymmetric structure in the initial TC vortex is important for accurate prediction of TC intensity, especially in the presence of large-scale environmental VWS.

4. Conclusions

This study conducted idealized high-resolution numerical experiments to help understand the possible effect of the asymmetric structure in the initial TC vortex on TC intensity changes at different developing stages in response to an imposed moderate environmental VWS. In all VWS experiments, the TC intensity responses to the imposed easterly VWS and westerly VWS are similar if the initial TC vortex was axisymmetric. In these VWS experiments, the wavenumber-1 asymmetric structure developed with upward motion downshear and downshear-left and subsidence upshear and upshear-right as documented in many previous studies. In experiments with asymmetric structure of the initial TC vortex, when the initial asymmetric structure was in phase with the VWS-induced asymmetric structure, the weakening would be enhanced and immediate after the VWS was imposed. However, when the two asymmetric structures are out of phase, the weakening would be suppressed compared with the TC in the experiments with the initial axisymmetric TC vortex. We have repeated our experiments using different initial vortex intensities for CTRL, and our results were consistent (Figure S2).

Our finding can help explain the results recently reported in Zhong et al. (2023), who found that the low-wavenumber components in the initial wind speed had played an important role in the initial spinup and spindown of the TC intensity in their ensemble prediction of Hurricane Patricia (2015) but the involved physical process was not explored. Our results suggest that the spinup and spindown could be partly due to the phasing between the initial TC vortex asymmetry and that induced by the environmental VWS in their ensemble simulations, because they also noticed the presence of large-scale moderate environmental VWS in Hurricane Patricia case. Our results also support that the initial TC weakening in response to the imposed moderate VWS is qualitatively proportional to the degree of the asymmetry of the TC vortex while the actual weakening rate also depends on the initial TC intensity. Therefore, this study demonstrates that it is key to accurately represent the asymmetric structure of the initial TC vortex in numerical models for skillful prediction of TC intensity. Our results also call for efforts in improving the observations of asymmetric structure in TCs and understanding effect of the asymmetric structure on TC intensity change. Note that a detailed physical process analysis of the TC intensity change in response to an imposed environmental VWS at the different TC developing stages is planned for a future study.

Acknowledgments

The authors thank Prof. Qingqing Li and Dr. Jianfeng Gu for their helpful discussions in this study. Q. Gao was supported by National Natural Science Foundation of China under grant 41730960 and Y. Wang was supported by NSF grant AGS-1834300.

Data Availability Statement

The WRF simulations were conducted using the WRF model Version 4.2.2, which were downloaded from the website (https://github.com/wrf-model/WRF/releases). All simulation data that support the findings of this study are available at https://datadryad.org/stash/share/5NMoeWi9hITh5yBO3f7M7niYQ3708gP5BACM6KnV8zY.

References

Bryan, G. H., & Rotunno, R. (2009a). The influence of near-surface, high-entropy air in hurricane eyes on maximum hurricane intensity. *Journal of the Atmospheric Sciences, 66*(1), 148–158. https://doi.org/10.1175/2008JAS2707.1

Bryan, G. H., & Rotunno, R. (2009b). Evaluation of an analytical model for the maximum intensity of tropical cyclones. *Journal of the Atmospheric Sciences, 66*(10), 3042–3060. https://doi.org/10.1175/2009JAS3038.1

Charney, J. G., & Eliassen, A. (1964). On the growth of the hurricane depression. *Journal of the Atmospheric Sciences*, *21*(1), 68–75. https://doi.org/10.1175/1520-0469(1964)021<0068:OTGOTH>2.0.CO;2

Cha, D. -H., & Wang, Y. (2013). A dynamical initialization scheme for real-time forecasts of tropical cyclones using the WRF model. *Monthly Weather Review*, *141*(3), 964–986. https://doi.org/10.1175/MWR-D-12-00077.1

Dunion, J. P. (2011). Rewriting the climatology of the tropical north Atlantic and Caribbean Sea atmosphere. *Journal of Climate*, *24*(3), 893–908. https://doi.org/10.1175/2010JCLI3496.1

Emanuel, K. A. (1986). An air-sea interaction theory for tropical cyclones. Part I: Steady-state maintenance. *Journal of the Atmospheric Sciences, 43*(6), 585-605. https://doi.org/10.1175/1520-0469(1986)043<0585:AASITF>2.0.CO;2

Emanuel, K. A. (2012). Self-stratification of tropical cyclone outflow: Part II: Implications to storm intensification. Journal of the Atmospheric Sciences, *69*(3), 988–996. https://doi.org/10.1175/JAS-D-11-0177.1

Emanuel, K. A., Desautels, C., Holloway, C., & Korty, R. (2004). Environmental control of tropical cyclone intensity. *Journal of the Atmospheric Sciences*, *61*(7), 843-858. https://doi.org/10.1175/1520-0469(2004)061<0843:ECOTCI>2.0.CO;2

Frank, W. M., & Ritchie, E. A. (2001). Effects of vertical wind shear on the intensity and structure of numerically simulated hurricanes. *Monthly Weather Review*, *129*(9), 2249–2269. https://doi.org/10.1175/1520-0493(2001)129<2249:EOVWSO>2.0.CO;2

Fu, H., Wang, Y., Riemer, M., & Li, Q.-Q. (2019). Effect of unidirectional vertical wind shear on tropical cyclone intensity change – Lower-layer shear versus upper-layer shear. *Journal of Geophysical Research – Atmospheres, 124*(12)*,* 6265–6282. https://doi.org/10.1029/2019JD030586

Gu, J.-F., Tan, Z.-M., & Qiu, X. (2018). The evolution of vortex tilt and vertical motion of tropical cyclones in directional shear flows. *Journal of the Atmospheric Sciences*, *75*(10), 3565–3578. https://doi.org/10.1175/JAS-D-18-0024.1

Gu, J.-F., Tan, Z.-M., & Qiu, X. (2019). Intensification variability of tropical cyclones in directional shear flows: vortex tilt–convection coupling. *Journal of the Atmospheric Sciences*, *76*(6), 1827–1844. https://doi.org/10.1175/JAS-D-18-0282.1

Gao, Q., Li, Q.-Q., & Dai, Y.-F. (2020). Characteristics of the outer rainband stratiform sector in numerically simulated tropical cyclones: Lower-layer shear versus upper-layer shear. *Advances in Atmospheric Sciences*, *37*(4), 399–419. https://doi.org/10.1007/s00376-020-9202-y

He, F., Posselt, D. J., Zarzycki, C. M., & Jablonowski, C. (2015). A balanced tropical cyclone test case for Agcms with background vertical wind shear. *Monthly Weather Review*, *143*(5), 1762–1781. https://doi.org/10.1175/MWR-D-14-00366.1

Heymsfield, G. M., Simpson, J., Halverson, J., Tian, J., Ritchie, E., & Molinari, J. (2006). Structure of highly sheared tropical storm Chantal during CAMEX-4. *Journal of the Atmospheric Sciences*, *63*(1), 268–287. https://doi.org/10.1175/JAS3602.1

Hong, S.-Y., Noh, Y., & Dudhia, J. (2006). A new vertical diffusion package with an explicit treatment of entrainment processes. *Monthly Weather Review*, *134*(9), 2318–2341. https://doi.org/10.1175/MWR3199.1

Jones, S. C. (1995). The evolution of vortices in vertical shear. Part I: Initially barotropic vortices. *Quarterly Journal of the Royal Meteorological Society*, *121*(524), 821–851. https://doi.org/10.1002/qj.49712152406

Li, Q.-Q., Duan, Y.-H., Yu, H., & Fu, G. (2008). A high-resolution simulation of Typhoon Rananim (2004) with MM5. Part I: Model verification, inner-core shear, and asymmetric convection. *Monthly Weather Review*, *136*(7), 2488−2506. https://doi.org/10.1175/2007MWR2159.1

Li, Q.-Q., & Dai, Y.-F. (2019). Revisiting azimuthally asymmetric moist instability in the outer core of sheared tropical cyclones. *Monthly Weather Review*, *148*(3), 1297−1319. https://doi.org/10.1175/MWR-D-19-0004.1

Li, Q.-Q., Wang, Y., & Duan, Y.-H. (2017). A numerical study of outer rainband formation in a sheared tropical cyclone. *Journal of the Atmospheric Sciences*, *74*(1), 203–227. https://doi.org/10.1175/JAS-D-16-0123.1

Li, Y.-L., Wang, Y., & Lin, Y.-L. (2019). Revisiting the dynamics of eyewall contraction of tropical cyclones. *Journal of the Atmospheric Sciences*, *76*(10), 3229–3245. https://doi.org/10.1175/JAS-D-19-0076.1

Li, Y.-L., Wang, Y., & Lin, Y.-L (2020). How much does the upward advection of the supergradient component of boundary layer wind contribute to tropical cyclone intensification and maximum intensity? *Journal of the Atmospheric Sciences*, *77*(8), 2649–2664. https://doi.org/10.1175/JAS-D-19-0350.1

Li, Y.-L., Wang, Y., Lin, Y.-L., & Wang, X. (2021). Why does rapid contraction of the radius of maximum wind precede rapid intensification in tropical cyclones? *Journal of the Atmospheric Sciences*, *78*(11), 3441–3453. https://doi.org/10.1175/JAS-D-21-0129.1

Li, Y.-L., Tan, Z.-M., & Wang, Y. (2022). Relative timing of the ends of hurricane intensification and contraction of the radius of maximum wind in the north Atlantic and Eastern north Pacific. *Geophysical Research Letters*, *49*(22), L101027. https://doi.org/10.1029/2022GL101027

Liu, H.-Y, Wang, Y., Xu, J., & Duan, Y. -H. (2018). A dynamical initialization scheme for tropical cyclones under the influence of terrain. *Weather and forecasting*, *33*(3), 641–659. https://doi.org/10.1175/WAF-D-17-0139.1

Liu, L., Wang, Y., & Duan, Y. -H. (2019). Contribution of Recycling of Surface Precipitation to Landfalling Tropical Cyclone Rainfall: A Modeling Study for Typhoon Utor (2013). *Journal of Geophysical Research – Atmospheres*, *124*(2), 870–885. https://doi.org/10.1029/2018JD029380

Montgomery, M. T., Nicholls, M. E., Cram, T. A., & Saunders, A. B. (2006). A vortical hot tower route to tropical cyclogenesis. *Journal of the Atmospheric Sciences*, *63*(1), 355-386. https://doi.org/10.1175/JAS3604.1

Montgomery, M. T., & Smith, R. K. (2014). Paradigms for tropical cyclone intensification. *Australian*

Meteorological and Oceanographic Journal, (Bruce Morton Memorial Volume), *64*, 37–66.

Nolan, D. S., Moon, Y. & Stern, D. P. (2007). Tropical cyclone intensification from asymmetric convection: Energetics and efficiency. *Journal of the Atmospheric Sciences*, *64*(10), 3377–3405. https://doi.org/10.1175/JAS3988.1

Ooyama, K. V. (1969). Numerical simulation of the life cycle of tropical cyclones. *Journal of the Atmospheric Sciences*, *26*(1), 3–40. https://doi.org/10.1175/1520-0469(1969)026<0003:NSOTLC>2.0.CO;2

Persing, J., Montgomery, M. T., McWilliams, J. C., & Smith, R. K. (2013). Asymmetric and axisymmetric dynamics of tropical cyclones. *Atmospheric Chemistry Physics*, *13*(24), 12299–12341. https://doi.org/10.5194/acp-13-12299-2013

Riemer, M., & Montgomery M. T. (2011). Simple kinematic models for the environmental interaction of tropical cyclones in vertical wind shear. *Atmospheric Chemistry and Physics*, *11*(17), 9395–9414. https://doi.org/10.5194/acp-11-9395-2011

Ritchie, E. A., & Frank, W. M. (2007). Interactions between simulated tropical cyclones and an environment with a variable Coriolis parameter. *Monthly Weather Review*, *135*(5), 1889–1905. https://doi.org/10.1175/MWR3359.1

Rotunno, R., & Emanuel, K. A. (1987). An air-sea interaction theory for tropical cyclones. Part II: Evolutionary study using a nonhydrostatic axisymmetric numerical model. *Journal of the Atmospheric Sciences*, *44*(3), 542–561. https://doi.org/10.1175/1520-0469(1987)044<0542:AAITFT>2.0.CO;2

Schubert, W. H., & Hack, J. J. (1982). Inertial stability and tropical cyclone development. *Journal of the Atmospheric Sciences,* *39*(8), 1687-1697. https://doi.org/10.1175/1520-0469(1982)039<1687:ISATCD>2.0.CO;2

Skamarock, W. C., Klemp, J. B., Dudhia, J., Gill, D. O., Barker, D. M., Duda, M. G., Huang, X. Y., Wang, W., & Powers, J. G. (2008). A description of the advanced research WRF version 3. *NCAR Tech. Note NCAR/TN-4751STR*, *113*. [Available online at http://www.mmm.ucar.edu/wrf/users/docs/ arw_v3_bw.pdf.]

Thompson, G., Field, P. R., Rasmussen, R. M., & Hall, W. D. (2008). Explicit forecasts of winter precipitation using an improved bulk microphysics scheme. Part II: Implementation of a new snow parameterization. *Monthly Weather Review*, *136*(12), 5095–5115. https://doi.org/10.1175/2008MWR2387.1

Tiedtke, M. (1989). A comprehensive mass flux scheme for cumulus parameterization in large-scale models. *Monthly Weather Review*, *117*(8), 1779–1800. https://doi.org/10.1175/1520-0493(1989)117<1779:ACMFSF>2.0.CO;2

Wang, Y. (2002a). Vortex Rossby waves in a numerically simulated tropical cyclone. Part I: Overall structure, potential vorticity and kinetic energy budgets. *Journal of the Atmospheric Sciences, 59*(7), 1213–1238. https://doi.org/10.1175/1520-0469(2002)059<1213:VRWIAN>2.0.CO;2

Wang, Y. (2002b). Vortex Rossby waves in a numerically simulated tropical cyclone. Part II: The role in tropical cyclone structure and intensity changes. *Journal of the Atmospheric Sciences, 59*(7), 1239–1262. https://doi.org/10.1175/1520-0469(2002)059<1239:VRWIAN>2.0.CO;2

Wang, Y. (2007). A multiply nested, movable mesh, fully compressible, nonhydrostatic tropical cyclone model - TCM4: Model description and development of asymmetries without explicit asymmetric forcing. *Meteorology and Atmospheric Physics*, *97*, 93–116. https://doi.org/10.1007/s00703-006-0246-z

Wang, Y. (2009). How do outer spiral rainbands affect tropical cyclone structure and intensity? *Journal of the Atmospheric Sciences*, *66*(5), 1250–1273. https://doi.org/10.1175/2008JAS2737.1

Wang. Y., & Holland, G. J. (1996a). Tropical cyclone motion and evolution in vertical shear. *Journal of the Atmospheric Sciences*, *53*(22), 3313–3332. https://doi.org/10.1175/1520-0469(1996)053,3313:TCMAEI.2.0.CO;2

Wang Y**.**, & Holland, G. J. (1996b). The beta drift of baroclinic vortices. Part II: Diabatic vortices. *Journal of the Atmospheric Sciences,* *53*(24), 3737–3756. https://doi.org/10.1175/1520-0469(1996)053<3737:TBDOBV>2.0.CO;2

Wang, Y., & Holland, J. G. (1996c). The beta drift of baroclinic vortices. Part I: Adiabatic vortices. *Journal of the Atmospheric Sciences,* *53*(3), 411–427. https://doi.org/10.1175/1520-0469(1996)053<0411:TBDOBV>2.0.CO;2

Wang, Y., & Wu, C.-C. (2004). Current understanding of tropical cyclone structure and intensity changes-A review. *Meteorology and. Atmospheric Physics*, *87*, 257–278. https://doi.org/10.1007/s00703-003-0055-6

Wang, Y., Li, Y.-L., Xu, J., Tan, Z.-M., & Lin, Y.-L. (2021a). The intensity-dependence of tropical cyclone intensification rate in a simplified energetically based dynamical system model. *Journal of the Atmospheric Sciences*, *78*(7), 2033–2045. https://doi.org/10.1175/JAS-D-20-0393.1

Wang, Y., Li, Y., & Xu, J. (2021b). A new time-dependent theory of tropical cyclone intensification. *Journal of the Atmospheric Sciences*, *78*(12), 3855–3865. https:/doi.org/10.1175/JAS-D-21-0169.1

Wang, Y., Tan, Z.-M. & Li, Y.-L., (2023). Some refinements to the most recent simple time-dependent theory of tropical cyclone intensification and sensitivity. *Journal of the Atmospheric Sciences*, *79*(1), 321–335. https://doi.org/10.1175/JAS-D-22-0135.1

Xu, Y.-M., & Wang, Y. (2013). On the initial development of asymmetric vertical motion and horizontal relative flow in a mature tropical cyclone embedded in environmental vertical shear. *Journal of the Atmospheric Sciences*, *70*(11), 3471–3491. https://doi.org/10.1175/JAS-D-12-0335.1

Yang, B., Wang, Y. & Wang, B. (2007). The effect of internally generated inner-core asymmetries on tropical cyclone potential intensity. *Journal of the Atmospheric Sciences*, *64*(4), 1165–1188. https://doi.org/10.1175/JAS3971.1

Zhang, C.-X., Wang, Y., & Hamilton, K. (2011). Improved representation of boundary layer clouds over the southeast Pacific in ARW-WRF using a modified Tiedtke cumulus parameterization scheme. *Monthly Weather Review*, *139*(11), 3489–3513. https://doi.org/10.1175/MWR-D-10-05091.1

Zeng, Z., Wang, Y. & Chen, L.-S. (2010). A statistical analysis of vertical shear effect on tropical cyclone intensity change in the north Atlantic: Vertical shear effect on TC intensity. *Geophysical Research Letters*, *37*(2), L02802. https://doi.org/10.1029/2009GL041788

Zhong, Q.-J., Wang, W.-G., Ding, R.-Q., Lu, X., Huang, Y.-J., Duan, W.-S., Liu, L. (2023). Impact of the low wavenumber structure in the initial vortex wind analyses on the prediction of the intensification of Hurricane Patricia (2015). *Journal of Geophysical Research – Atmospheres*, *128*(2), e2022JD037082. https://doi.org/10.1029/2022JD037082